AIAA JOURNAL
Vol. 53, No. 10, October 2015

Finite Element Formulation Based on the Extended High-Order Sandwich Panel Theory

Zhangxian Yuan* and George A. Kardomateas†
Georgia Institute of Technology, Atlanta, Georgia 30332-0150
and
Yeoshua Frostig‡
Technion–Israel Institute of Technology, 32000 Haifa, Israel

DOI: 10.2514/1.J053736

The extended high-order sandwich panel theory was formulated in its one-dimensional version for orthotropic elastic sandwich beams. This theory includes the in-plane rigidity of the core, and the compressibility of the soft core in the transverse direction is also considered. The novelty of this theory is that it allows for three generalized coordinates in the core (the axial and transverse displacements at the centroid of the core, and the rotation at the centroid of the core) instead of just one (midpoint transverse displacement) commonly adopted in other available theories. The theory was derived so that all core/face displacement continuity conditions are fulfilled. It is proven, by comparison to the elasticity solution, that this approach results in superior accuracy, especially for the cases of stiffer cores, for which cases of the other available sandwich computational models cannot correctly predict the stress fields involved. In this paper, a linear finite element is formulated based on the extended high-order sandwich panel theory. The element equations are outlined, and numerical results for the simply supported case of transverse distributed loading are produced for several typical sandwich configurations. These results are compared with the corresponding ones from the elasticity solution. The comparison among these numerical results shows that, with a relatively small number of elements, the results are very close to the elasticity ones in terms of both the displacements and stress or strains. Thus, the finite element version of the extended high-order sandwich panel theory constitutes a very powerful analytical tool for sandwich panels.

Nomenclature

a	=	length of the sandwich beam, m
C_{ij}	=	stiffness constants, N/m^2
c	=	half-thickness of the core (total core thickness is $2c$), m
$f_{t,b}$	=	thickness of the top face and bottom face, respectively, m
$[K_e^{t,b,c}]$	=	element unit width stiffness matrix of the top face, bottom face, and core, N/m^2
$[N(s)]$	=	displacement interpolation matrix
$N_k(s)$	=	shape functions (where k is equal to $1,\ldots,6$)
$\{R_e^{t,b,c}\}$	=	element unit width equivalent nodal load vector of the top face, bottom face, and core, N/m
s	=	local coordinate
$\{\boldsymbol{U}_e\}$	=	column nodal displacement matrix of the element, m
$\{\tilde{U}(s)\}$	=	column matrix representing the displacement field within the element, m
u	=	axial displacement (along x), m
w	=	transverse displacement (along z), m

Introduction

SANDWICH panels typically consist of two stiff metallic or composite thin face sheets separated by a soft/stiff honeycomb or foam thick core of low/high density. This configuration gives the sandwich material system high stiffness and strength with little resultant weight penalty and high-energy absorption capability related to the application of sandwich structures in the construction of aerospace vehicles, naval vehicles, wind turbines, and civil infrastructure. There are several distinguishing features of sandwich panels with regard to the analysis of their static and dynamic behavior. One is the large effect of transverse shear [1]. This is because cores are typically of very low modulus, and thus transverse shear has a significant influence on the structural behavior. Another very important feature is the compressibility of the core, which results in significant core transverse deformation. The latter has been shown in experiments on sandwich panels subject to impulsive (blast) loading [2]. Consideration of the core compressibility implies that the displacements of the upper and lower face sheets may not be identical.

The earliest models of sandwich analysis are the classical or first-order shear models, which assume that the core is infinitely rigid (incompressible) in its transverse direction, its in-plane rigidity is neglected, and it has only shear resistance. In general, they are based on the Euler–Bernoulli and Timoshenko beam theories with modulus-weighted stiffnesses. This model has been shown to be inaccurate in predicting displacements for very soft-core sandwich configurations under quasi-static loading (Kardomateas and Phan [3]). In 1992, Frostig et al. [4] developed the high-order sandwich panel theory (HSAPT), which is a compressible core theory that accounts for the transverse and shear rigidity of the core but neglects the axial rigidity of the core. Neglecting the axial rigidity of the core results in a constant shear stress distribution through the thickness of the core, which is a good approximation for sandwich constructions with very soft cores undergoing quasi-static loading [3]. Recently, the extended high-order sandwich panel theory (EHSAPT) was formulated to account for the axial, transverse, and shear rigidity of the core (Phan et al. [5]). This new theory includes the axial rigidity of the core and allows for an accurate prediction of the shear stress distribution through the thickness of the core in a wide range of core stiffnesses [5]. The dynamic version of the EHSAPT was derived and presented by Phan et al. [6]. It was validated by comparison to the dynamic elasticity solution derived by Kardomateas et al. [7]. Another category of theories includes the so-called "zigzag" theories. These theories were original developed for laminated composites. In the zigzag theories, the displacements have a piecewise variation through the thickness. The shear stress is continuous at the layer interfaces.

Received 24 August 2014; revision received 13 February 2015; accepted for publication 19 February 2015; published online 19 May 2015.

*Doctoral Student and Graduate Research Assistant.
†Professor of Aerospace Engineering.
‡Professor of Structural Engineering.

During the years, a number of zigzag models have been developed [8–9]. Recently, a"refined zigzag theory" was proposed by Barut and Madenci [8]. The in-plane and transverse displacement components have a quadratic through-thickness variation, and the transverse normal strain is obtained through the assumption of a cubic variation of the transverse normal stress. Also recently, Iurlaro et al. [9] developed a mixed cubic zigzag model for multilayered composite and sandwich plates. The in-plane displacements follow a piecewise cubic distribution, and the transverse displacement has a parabolic variation through thickness. The assumed transverse shear stress profile comes from the three-dimensional equilibrium equations. These recent theories were shown to offer improvements, especially for thick or highly heterogeneous laminate configurations.

Direct solutions based on the EHSAPT can be obtained for simple configurations, such as the simply supported sandwich beam under sinusoidal transverse loading treated in [5]. For general and more complicated geometric and loading configurations, a direct solution of the theory is not always available; thus, the more general finite element formulations are needed. In fact, finite element formulations for sandwich structures have been pursued in the literature for both static and dynamic applications, based on different assumptions [10–16]: for example, [13] is based on the high-order sandwich panel theory. In [15], a new finite element (FE) model was built according to the higher-order zigzag theory. More recently, a triangular plate element based on {2,2}-order refined zigzag plate theory was developed [16].

Thus, the objective of the present work is to formulate a finite element based on the EHSAPT. The element formulation is outlined in detail. Three examples with various boundary conditions and applied loadings are investigated. To verify the formulations and solutions, comparisons are made with analytical solutions obtained by elasticity and the EHSAPT. It is verified that the element is capable of handling complex end fixity and geometry configurations for a range of material systems. The EHSAPT element is shown to be a very efficient way of analyzing sandwich beam configurations with accuracy.

Theory and Derivation

The finite element formulation follows the new sandwich plate theory EHSAPT [5]. For completeness, the EHSAPT is briefly presented. In sandwich materials, the core is usually much thicker than the face sheets and of very low modulus; thus, the shear deformation plays an important role. The EHSAPT also includes the transverse compressibility as well as the axial rigidity of the core. Higher-order terms are needed to accurately describe the deformation of the core sheet.

Consider a sandwich beam or wide panel consisting of two face sheets bonded to a core, as shown in Fig. 1. The thickness of the top face sheet, bottom face sheet, and core sheet are f_t, f_b, and $2c$, respectively. The length of the beam/wide panel is a. The origin of a right-handed Cartesian coordinate is at the left end, the x axis coincides with the middle line of the core, and the z axis is in the thickness direction. As a plane strain problem, we only consider loading in the x-z plane, and this will result in displacements in the x and z directions. The x and z coordinate components of the displacement are denoted with u and w, respectively.

In typical sandwich panels, the geometric and material properties are very different between the skins and the core. The thickness ratio of the face sheets and core is very small, and the Young's modulus of the core is much smaller than that of the skins. For the face sheets, the axial strain is the major part, whereas the shear strain can be neglected. For the core, the axial strain, transverse strain, and shear strain need to all be considered. Hence, the displacement field in the face sheets is assumed to follow the Euler–Bernoulli assumptions, whereas a high-order displacement pattern is assumed for the core. In the EHSAPT, the core transverse displacement $w(x, z)$ is assumed to be a quadratic function of z and the axial displacement $u(x, z)$ is described by a cubic function of z. The transverse displacement can be expressed as

$$w(x,z) = \begin{cases} w_0^t(x) & (c < z \le c + f_t)\ \text{[top face]} \\ w_0^c(x) + w_1^c(x)z + w_2^c(x)z^2 & (-c \le z \le c)\ \text{[core]} \\ w_0^b(x) & (-c - f_b \le z < -c)\ \text{[bottom face]} \end{cases} \tag{1}$$

and the axial displacement as

$$u(x,z) = \begin{cases} u_0^t(x) - \left(z - c - \frac{f_t}{2}\right) w_{0,x}^t(x) & (c < z \le c + f_t)\ \text{[top face]} \\ u_0^c(x) + \phi_0^c(x)z + u_2^c(x)z^2 + u_3^c(x)z^3 & (-c \le z \le c)\ \text{[core]} \\ u_0^b(x) - \left(z + c + \frac{f_b}{2}\right) w_{0,x}^t(x) & (-c - f_b \le z < -c)\ \text{[bottom face]} \end{cases} \tag{2}$$

where, $w_0^t(x)$, $w_0^c(x)$, and $w_0^b(x)$ are the transverse displacements of the centerline of the top face, core, and bottom face, respectively. Similarly, $u_0^t(x)$, $u_0^c(x)$, and $u_0^b(x)$ are the axial displacements of the centerline of the top face, core, and bottom face, respectively. Also, $\phi_c(x)$ is the slope at the centroid of the core. These unknown quantities are functions of the x coordinate. For convenience, they will be denoted as w_0^k, u_0^k $(k = t, b, c)$, and ϕ^c.

The displacement continuity condition at the interfaces between the face sheets and the core allows solving for w_1^c, w_2^c, u_2^c, and u_3^c; thus, the displacement field is

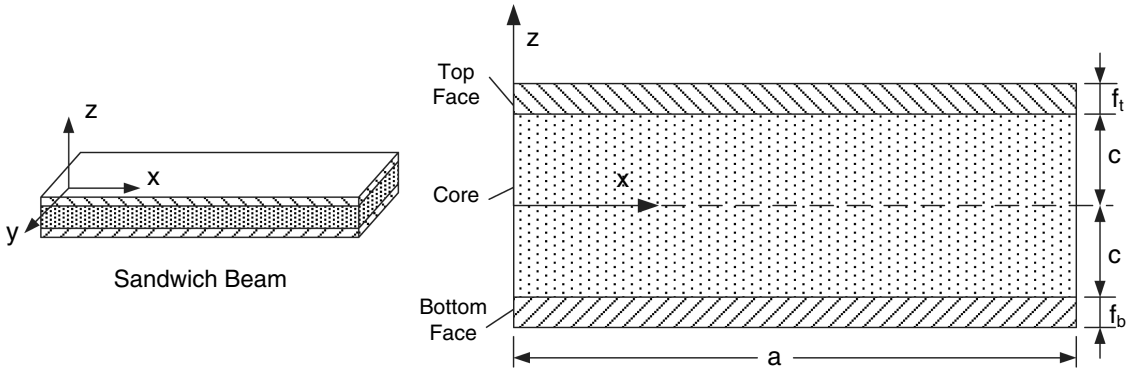

Fig. 1 Definition of the geometry and coordinate system for the sandwich beam/wide plate.

$$w(x,z)=\begin{cases} w_0^t(x) & (c<z\le c+f_t)\ \text{[top face]} \\ \left(\frac{z}{2c}+\frac{z^2}{2c^2}\right)w_0^t+\left(1-\frac{z^2}{c^2}\right)w_0^c++\left(-\frac{z}{2c}+\frac{z^2}{2c^2}\right)w_0^b & (-c\le z\le c)\ \text{[core]} \\ w_0^b(x) & (-c-f_b\le z<-c)\ \text{[bottom face]} \end{cases} \tag{3}$$

and

$$u(x,z)=\begin{cases} u_0^t(x)-\left(z-c-\frac{f_t}{2}\right)w_{0,x}^t(x) & (c<z\le c+f_t)\ \text{[top face]} \\ \frac{z^2}{2c^2}\left(1+\frac{z}{c}\right)u_0^t+\frac{f_t z^2}{4c^2}\left(1+\frac{z}{c}\right)w_{0,x}^t+\left(1-\frac{z^2}{c^2}\right)u_0^c+ & \\ +z\left(1-\frac{z^2}{c^2}\right)\phi_0^c+\frac{z^2}{2c^2}\left(1-\frac{z}{c}\right)u_0^b+\frac{f_b z^2}{4c^2}\left(-1+\frac{z}{c}\right)w_{0,x}^b & (-c\le z\le c)\ \text{[core]} \\ u_0^b(x)-\left(z+c+\frac{f_b}{2}\right)w_{0,x}^t(x) & (-c-f_b\le z<-c)\ \text{[bottom face]} \end{cases} \tag{4}$$

Applying the linear strain-displacement relationship

$$\epsilon_{xx}(x,z)=\frac{\partial u(x,z)}{\partial x};\qquad \epsilon_{zz}(x,z)=\frac{\partial w(x,z)}{\partial z};$$
$$\gamma_{xz}(x,z)=\frac{\partial u(x,z)}{\partial z}+\frac{\partial w(x,z)}{\partial x} \tag{5}$$

the strain components in the entire sandwich panel can be expressed in terms of the displacements of the centerline. As a consequence of the Euler-Bornoulli assumptions in the faces, the transverse normal strain and shear strain in the top and bottom faces, $\epsilon_{zz}^{t,b}$ and $\gamma_{xz}^{t,b}$, vanish. The axial strain $\epsilon_{xx}^{t,b}$ is the only nonzero strain in the top and bottom face sheets:

$$\epsilon_{xx}^t=u_{0,x}^t-\left(z-c-\frac{f_t}{2}\right)w_{0,xx}^t\qquad (c<z\le c+f_t),\qquad \text{[top face]} \tag{6a}$$

$$\epsilon_{xx}^b=u_{0,x}^b-\left(z+c+\frac{f_b}{2}\right)w_{0,xx}^b\quad (-c-f_b\le z<-c).\quad \text{[bottom face]} \tag{6b}$$

In the core, all strain components exist, and these are

$$\epsilon_{xx}^c=\frac{z^2}{2c^2}\left(1+\frac{z}{c}\right)u_{0,x}^t+\frac{f_t z^2}{4c^2}\left(1+\frac{z}{c}\right)w_{0,xx}^t+\left(1-\frac{z^2}{c^2}\right)u_{0,x}^c+$$
$$+z\left(1-\frac{z^2}{c^2}\right)\phi_{0,x}^c+\frac{z^2}{2c^2}\left(1-\frac{z}{c}\right)u_{0,x}^b+\frac{f_b z^2}{4c^2}\left(-1+\frac{z}{c}\right)w_{0,xx}^b \tag{7a}$$

$$\epsilon_{zz}^c=\left(\frac{z}{c^2}+\frac{1}{2c}\right)w_0^t-\frac{2z}{c^2}w_0^c+\left(\frac{z}{c^2}-\frac{1}{2c}\right)w_0^b \tag{7b}$$

$$\gamma_{xz}^c=\left(\frac{z}{c^2}+\frac{3z^2}{2c^3}\right)u_0^t+\left[\left(\frac{c+f_t}{2c^2}\right)z+\left(\frac{2c+3f_t}{4c^3}\right)z^2\right]w_{0,x}^t$$
$$-\frac{2z}{c^2}u_0^c+\left(1-\frac{3z^2}{c}\right)\phi_0^c+$$
$$+\left(1-\frac{z^2}{c^2}\right)w_{0,x}^c+\left(\frac{z}{c^2}-\frac{3z^2}{2c^3}\right)u_0^b$$
$$+\left[-\left(\frac{c+f_b}{2c^2}\right)z+\left(\frac{2c+3f_b}{4c^3}\right)z^2\right]w_{0,x}^b \tag{7c}$$

Equations (6) and (7) can be written in matrix form:

$$\{\boldsymbol{\epsilon}^t\}=[L^t]\{\bar{\boldsymbol{U}}\},\qquad \{\boldsymbol{\epsilon}^b\}=[L^b]\{\bar{\boldsymbol{U}}\},\qquad \{\boldsymbol{\epsilon}^c\}=[L^c]\{\bar{\boldsymbol{U}}\} \tag{8}$$

where $\{\boldsymbol{\epsilon}^{t,b,c}\}=[\,\epsilon_{xx}^{t,b,c}\quad \epsilon_{zz}^{t,b,c}\quad \gamma_{xz}^{t,b,c}\,]^T$ is the strain vector in the top face, bottom face, and core, respectively; and $\{\bar{\boldsymbol{U}}\}=[\,u_0^t\quad w_0^t\quad u_0^b\quad w_0^b\quad u_0^c\quad w_0^c\quad \phi_0^c\,]^T$ is the displacement vector. Also, $[L^{t,b,c}]$ is the differential operator matrix.

The constitutive laws in the three sandwich layers are

$$\{\boldsymbol{\sigma}^t\}=[C^t]\{\boldsymbol{\epsilon}^t\};\qquad \{\boldsymbol{\sigma}^b\}=[C^b]\{\boldsymbol{\epsilon}^b\};\qquad \{\boldsymbol{\sigma}^c\}=[C^c]\{\boldsymbol{\epsilon}^c\} \tag{9}$$

where $\{\boldsymbol{\sigma}^{t,b,c}\}=[\,\sigma_{xx}^{t,b,c}\quad \sigma_{zz}^{t,b,c}\quad \tau_{xz}^{t,b,c}\,]^T$ is the stress vector of the top face, bottom face, and core, respectively. The $[C^{t,b,c}]$ is the elastic modulus matrix corresponding to the top face, bottom face, and core.

We assume orthotropic material for all three sheets and, in this case, the elastic modulus matrix $C^{t,b,c}$ is given as

$$[C^{t,b,c}]=\begin{bmatrix} C_{11}^{t,b,c} & C_{13}^{t,b,c} & 0 \\ C_{13}^{t,b,c} & C_{33}^{t,b,c} & 0 \\ 0 & 0 & C_{55}^{t,b,c} \end{bmatrix} \tag{10}$$

where we have denoted $1\equiv x$, $3\equiv z$, and $55\equiv xz$.

Due to zero transverse normal strain and transverse shear strain in the top and bottom face sheets, $\sigma_{zz}^{t,b}$ and $\gamma_{xz}^{t,b}$ are equal to zero. So, the $C_{33}^{t,b}$ and $C_{55}^{t,b}$ will not come into the relationships for the face sheets. The rest of the stiffness parameters are given directly in terms of the elastic moduli and Poisson's ratio by $C_{11}^{t,b}=E_1^{t,b}$ and $C_{13}^{t,b}=\nu_{32}^{t,b}E_3^{t,b}$. In the orthotropic core, the terms of the $[C^c]$ matrix come from the inverse of the compliance matrix of the orthotropic material. However, only the C_{11}^c, C_{33}^c, C_{55}^c, and C_{13}^c are needed in the theory. This way of determining the stiffness constants of the core is slightly different than the way these were derived in [5], but the present approach shows improved accuracy of the EHSAPT by comparison to the Elasticity solution:

$$\begin{bmatrix} C_{11}^c & C_{12}^c & C_{13}^c & 0 & 0 & 0 \\ C_{12}^c & C_{22}^c & C_{23}^c & 0 & 0 & 0 \\ C_{13}^c & C_{23}^c & C_{33}^c & 0 & 0 & 0 \\ 0 & 0 & 0 & C_{44}^c & 0 & 0 \\ 0 & 0 & 0 & 0 & C_{55}^c & 0 \\ 0 & 0 & 0 & 0 & 0 & C_{66}^c \end{bmatrix}$$
$$=\begin{bmatrix} \frac{1}{E_1^c} & -\frac{\nu_{12}^c}{E_1^c} & -\frac{\nu_{13}^c}{E_1^c} & 0 & 0 & 0 \\ -\frac{\nu_{21}^c}{E_2^c} & \frac{1}{E_2^c} & -\frac{\nu_{23}^c}{E_2^c} & 0 & 0 & 0 \\ -\frac{\nu_{31}^c}{E_3^c} & -\frac{\nu_{32}^c}{E_3^c} & \frac{1}{E_3^c} & 0 & 0 & 0 \\ 0 & 0 & 0 & \frac{1}{G_{23}^c} & 0 & 0 \\ 0 & 0 & 0 & 0 & \frac{1}{G_{31}^c} & 0 \\ 0 & 0 & 0 & 0 & 0 & \frac{1}{G_{12}^c} \end{bmatrix}^{-1} \tag{11}$$

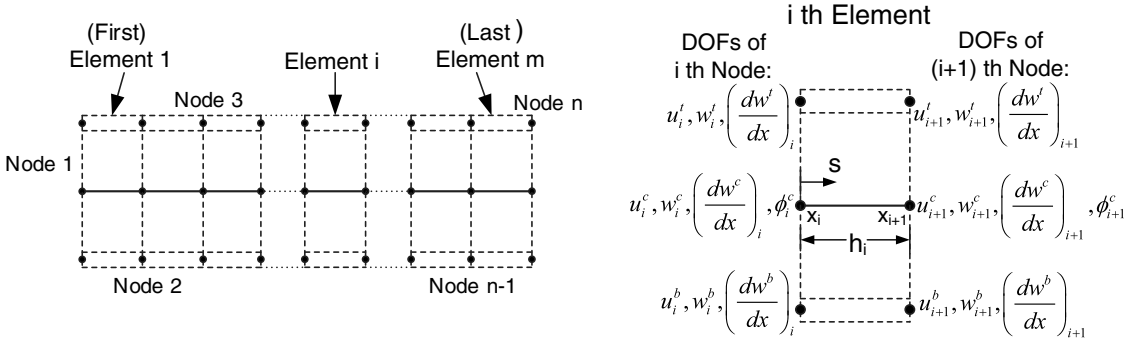

Fig. 2 Finite element model for a two-node element, $n = m + 1$.

Thus, all the strain and stress components of the sandwich beam/wide plate can be expressed in terms of the unknown displacement vector $\{\bar{U}\}$ according to the ESHAPT.

Finite Element Formulation

The EHSAPT contains high-order terms to describe the deformation of the sandwich cross section. As a result, the analytical solution is not easy to get; sometimes it does not even exist. On the other hand, the finite element method (FEM) is a commonly used numerical method in mechanics and can easily handle various combinations of loading and boundary conditions. Hence, we will use the EHSAPT to formulate a finite element and, in this way, develop a new simple, convenient, and accurate approach, which can have the advantages of both the EHSAPT and FEM, to simulate and predict the behavior of sandwich structures. To achieve this goal, an original sandwich element is formulated with 10 deg of freedom (DOFs) per "node." The node is actually a nodal line, since the DOFs are placed at different locations along the thickness direction, as shown in Fig. 2. Three of them are the transverse displacements of the midline of the top face, bottom face, and core, denoted as $w^{t,b,c}$. Another three DOFs are the first-order derivatives of $w^{t,b,c}$ with respect to the x coordinate, which are the $\mathrm{d}w^{t,b,c}/\mathrm{d}x$. Another three are the axial displacements of the midline of the top face, bottom face, and core, denoted as $u^{t,b,c}$. The last one is the rotation angle of the core's centerline ϕ^c. The proposed element contains both ϕ^c and $\mathrm{d}w^c/\mathrm{d}x$ as degrees of freedom. Although there is no direct physical meaning when considering the boundary condition corresponding to the term $\mathrm{d}w^c/\mathrm{d}x$, this term can be set free, meaning we can set its counterpart force equal to zero, at the boundaries. Numerical results will show that this formulation yields very accurate results, as compared to elasticity. It should be noted that the DOF of $\mathrm{d}w^c/\mathrm{d}x$ plays an important role to ensure the same shape function can be applied to the midline transverse displacement of the core and the face sheets. Otherwise, the core would exhibit a lower order of continuity between adjacent elements than the face sheets, and the midline deflection pattern of the core and face sheets would be inconsistent. If $\mathrm{d}w^c/\mathrm{d}x$ is not included, the deflection distribution of the core midline would be linear in each element and would only have C^0 continuity, whereas that of face sheets would be a cubic curve and would have C^1 continuity. The accuracy would be decreased dramatically, and this was observed in numerical experiments.

So, the displacement vector of the ith node is

$$\{\boldsymbol{U}_i\} = \left[u_i^t\ w_i^t \left(\frac{\mathrm{d}w^t}{\mathrm{d}x}\right)_i\ u_i^b\ w_i^b \left(\frac{\mathrm{d}w^b}{\mathrm{d}x}\right)_i\ u_i^c\ w_i^c \left(\frac{\mathrm{d}w^c}{\mathrm{d}x}\right)_i\ \phi_i^c\right]^T \tag{12}$$

The element may have several nodes, i.e., a two-node element, a three-node element, or even an element with more than three nodes can be formulated. For a p-node element, Lagrange interpolation polynomials of degree $p-1$ are used to interpolate the axial displacement field $\tilde{u}^{t,b,c}$ and the rotation angle of the core sheet $\tilde{\phi}^c$ within one element. For the transverse displacement field $\tilde{w}^{t,b,c}$, Hermite interpolating polynomials of degree $2p-1$ are used to ensure the C^1 continuity between adjacent elements. Considering that a two-node element is the simplest and easiest to use and (as proved later) of high accuracy, we shall formulate in the following such a two-node EHSAPT-based element as an example to illustrate the interpolation of a p-node element. The sandwich beam is divided into m elements and has a total of $n = m + 1$ nodes. Considering the ith element, the shape function of the displacement field for the two-node element is assumed to be

$$\begin{Bmatrix} \tilde{u}^t(s) \\ \tilde{w}^t(s) \\ \tilde{u}^b(s) \\ \tilde{w}^b(s) \\ \tilde{u}^c(s) \\ \tilde{w}^c(s) \\ \tilde{\phi}^c(s) \end{Bmatrix} = [N(s)] \begin{Bmatrix} \{\boldsymbol{U}_i\} \\ \{\boldsymbol{U}_{i+1}\} \end{Bmatrix} \tag{13a}$$

where

$$N(s) = \begin{bmatrix} N_1 & 0 & 0 & 0 & 0 & 0 & 0 & 0 & 0 & 0 & N_2 & 0 & 0 & 0 & 0 & 0 & 0 & 0 & 0 & 0 \\ 0 & N_3 & N_4 & 0 & 0 & 0 & 0 & 0 & 0 & 0 & 0 & N_5 & N_6 & 0 & 0 & 0 & 0 & 0 & 0 & 0 \\ 0 & 0 & 0 & N_1 & 0 & 0 & 0 & 0 & 0 & 0 & 0 & 0 & 0 & N_2 & 0 & 0 & 0 & 0 & 0 & 0 \\ 0 & 0 & 0 & 0 & N_3 & N_4 & 0 & 0 & 0 & 0 & 0 & 0 & 0 & 0 & N_5 & N_6 & 0 & 0 & 0 & 0 \\ 0 & 0 & 0 & 0 & 0 & 0 & N_1 & 0 & 0 & 0 & 0 & 0 & 0 & 0 & 0 & 0 & N_2 & 0 & 0 & 0 \\ 0 & 0 & 0 & 0 & 0 & 0 & 0 & N_3 & N_4 & 0 & 0 & 0 & 0 & 0 & 0 & 0 & 0 & N_5 & N_6 & 0 \\ 0 & 0 & 0 & 0 & 0 & 0 & 0 & 0 & 0 & N_1 & 0 & 0 & 0 & 0 & 0 & 0 & 0 & 0 & 0 & N_2 \end{bmatrix} \tag{13b}$$

In the preceding matrix, the shape functions $N_k(k = 1 \ldots 6)(s)$ are in terms of the local coordinate, $s = x - x_i$, where x_i is the x coordinate of the ith node (Fig. 2); also, in the following equations for the shape functions, $h_i = x_{i+1} - x_i$ is the length of the ith element:

$$N_1 = 1 - \frac{s}{h_i}; \qquad N_2 = \frac{s}{h_i} \tag{13c}$$

$$N_3 = 1\text{–}3\frac{s^2}{h_i^2} + 2\frac{s^3}{h_i^3}; \qquad N_4 = s - 2\frac{s^2}{h_i} + \frac{s^3}{h_i^2} \tag{13d}$$

$$N_5 = 3\frac{s^2}{h_i^2} - 2\frac{s^3}{h_i^3}; \qquad N_6 = -\frac{s^2}{h_i} + \frac{s^3}{h_i^2} \tag{13e}$$

For convenience, Eq. (13a) is expressed in matrix form:

$$\{\tilde{\boldsymbol{U}}(s)\} = [N(s)]\{\boldsymbol{U}_e\} \tag{14}$$

where $\{\boldsymbol{U}_e\}$ is a 20×1 column matrix representing the unknown displacement vector of the ith element (nodal displacements), and $[N(s)]$ is the 7×20 displacement interpolation matrix [see Eq. (13b)]. Also, $\{\tilde{U}(s)\}$ is the 7×1 column matrix representing the EHSAPT displacement field in the element at any point s.

Considering Eqs. (8) and (14), a strain interpolation matrix can be defined for the faces and the core as

$$[B^k] = [L^k][N(s)] \qquad k = t, b, c \tag{15a}$$

Thus, one has

$$\{\boldsymbol{\epsilon}^k\} = [B^k]\{\boldsymbol{U}_e\} \qquad k = t, b, c \tag{15b}$$

Applying the constitutive law [Eq. (9)], the stress in the top face $\{\boldsymbol{\sigma}^t\}$, bottom face $\{\boldsymbol{\sigma}^b\}$, and the core $\{\boldsymbol{\sigma}^c\}$ can be expressed in terms of the nodal displacement vector $\{\boldsymbol{U}_e\}$:

$$\{\boldsymbol{\sigma}^k\} = [C^k]\{\boldsymbol{\epsilon}^k\} = [C^k][B^k]\{\boldsymbol{U}_e\}, \qquad k = t, b, c \tag{15c}$$

The total potential energy per unit width of ith element is

$$\Pi^e = \int_0^{h_i}\left[\int_c^{c+f_t} \{\boldsymbol{\epsilon}^t\}^T\{\boldsymbol{\sigma}^t\}\,\mathrm{d}z + \int_{-c}^{c} \{\boldsymbol{\epsilon}^c\}^T\{\boldsymbol{\sigma}^c\}\,\mathrm{d}z + \int_{-c-f_b}^{-c} \{\boldsymbol{\epsilon}^b\}^T\{\boldsymbol{\sigma}^b\}\,\mathrm{d}z\right]\mathrm{d}s - W^e \tag{16}$$

where W^e is the work done by the external force. The element unit width stiffness matrix $[K_e]$ can be derived by applying the principle of minimum potential energy, i.e., by taking the first variation of Eq. (16) with respect to $\{\boldsymbol{U}_e\}$. The top face, the bottom face, and the core all contribute to the stiffness of the sandwich panel:

$$[K_e] = [K_e^t] + [K_e^c] + [K_e^b] \tag{17}$$

where $[K_e^t]$, $[K_e^c]$, and $[K_e^b]$ are the element stiffness matrices per unit width resulting from the top face, the core, and the bottom face, respectively. These can be computed explicitly as

$$[K_e^t] = \int_0^{h_i}\int_c^{c+f_t} [B^t]^T[C^t][B^t]\,\mathrm{d}z\,\mathrm{d}s \tag{18a}$$

$$[K_e^c] = \int_0^{h_i}\int_{-c}^{c} [B^c]^T[C^c][B^c]\,\mathrm{d}z\,\mathrm{d}s \tag{18b}$$

$$[K_e^b] = \int_0^{h_i}\int_{-c-f_b}^{-c} [B^b]^T[C^b][B^b]\,\mathrm{d}z\,\mathrm{d}s \tag{18c}$$

Various loads, such as concentrated forces, distributed forces, and moments, can be applied to the sandwich panel. All of these loads can be and need to be turned into generalized nodal forces (same as in the general finite element method). The element load vector can be obtained by taking the variation of the work done by the external forces W^e in Eq. (16). Let us consider the most general distributed loading case, and let us denote by $p^{t,c,b}$ the distributed axial force per unit width applied to the midsurface of the top face, core, and bottom face, as well as by $q^{t,c,b}$, which is the distributed transverse force per unit width applied to the midsurface of the top face, core, and bottom face. Also, by $m^{t,c,b}$, the distributed moment per unit width applied to the midsurface of the top face, core, and bottom face, respectively.

For consistency and convenience, let us introduce three differential operator matrices:

$$[A^t] = \begin{bmatrix} 1 & 0 & 0 & 0 & 0 & 0 & 0 \\ 0 & 1 & 0 & 0 & 0 & 0 & 0 \\ 0 & \frac{\partial}{\partial s} & 0 & 0 & 0 & 0 & 0 \end{bmatrix}; \qquad [A^c] = \begin{bmatrix} 0 & 0 & 0 & 0 & 1 & 0 & 0 \\ 0 & 0 & 0 & 0 & 0 & 1 & 0 \\ 0 & 0 & 0 & 0 & 0 & 0 & 1 \end{bmatrix};$$

$$[A^b] = \begin{bmatrix} 0 & 0 & 1 & 0 & 0 & 0 & 0 \\ 0 & 0 & 0 & 1 & 0 & 0 & 0 \\ 0 & 0 & 0 & \frac{\partial}{\partial s} & 0 & 0 & 0 \end{bmatrix} \tag{19}$$

The corresponding equivalent nodal loads at the top face, bottom face, and core can be explicitly computed as

$$\{\mathbf{R}_e^t\} = \int_0^{h_i} [N]^T[A^t]^T \begin{Bmatrix} p^t \\ q^t \\ m^t \end{Bmatrix} \mathrm{d}s; \qquad \{\mathbf{R}_e^c\} = \int_0^{h_i} [N]^T[A^c]^T \begin{Bmatrix} p^c \\ q^c \\ m^c \end{Bmatrix} \mathrm{d}s;$$

$$\{\mathbf{R}_e^b\} = \int_0^{h_i} [N]^T[A^b]^T \begin{Bmatrix} p^b \\ q^b \\ m^b \end{Bmatrix} \mathrm{d}s \tag{20}$$

where $\{\mathbf{R}_e^t\}$, $\{\mathbf{R}_e^c\}$, and $\{\mathbf{R}_e^b\}$ are the equivalent nodal concentrated loads per unit width resulting from the distributed loads of the top face, the core, and the bottom face sheet. Moreover, when concentrated forces or moments are applied at the center surface of the top face, core, and bottom faces (such as the axial forces denoted as $P^{t,c,b}$ per unit width, shear forces denoted as $V^{t,c,b}$ per unit width, or bending moments denoted as $M^{t,c,b}$ per unit width), these concentrated loads can be added directly to the load vector corresponding to the nodal displacement.

The element equivalent nodal concentrated load is the summation of the loads from the top face, bottom face, and core; thus, one has

$$\{\mathbf{R}_e\} = \{\mathbf{R}_e^t\} + \{\mathbf{R}_e^c\} + \{\mathbf{R}_e^b\} \tag{21}$$

Finally, the element equilibrium equation is given by

$$[K_e]\{\boldsymbol{U}_e\} = \{\mathbf{R}_e\} \tag{22}$$

Once the element stiffness matrix and element nodal loads are derived, the stiffness matrix and load vector of the entire sandwich beam/wide plate can be easily obtained by assembling all the elements.

Numerical Examples and Discussion of the Results

Computer programs are written, and static analyses of the sandwich beams subjected to various loadings and boundary conditions are presented. To verify the derivation of formulas and the solution procedures, some results are compared to results available in the literature and other theoretical results.

Example 1: Consider a simply supported sandwich beam subjected to a sinusoidal distributed load. For this particular case, the theoretical elasticity results are also available [3] for the geometrical parameters of $f_t = f_b = 2$ mm, $2c = 16$ mm, and $a = 400$ mm. The sandwich material configuration consists of graphite epoxy faces and glass phenolic honeycomb core, and the material properties are listed in Table 1. A distributed load $q^t = q_0 \sin(\pi x/a)$ is applied to the top face sheet. This configuration is analyzed with the two-node element described in the previous section. For further insight into this

Table 1 Material properties

	E_1	E_2	E_3	G_{23}	G_{31}	G_{12}	ν_{32}	ν_{31}	ν_{12}
Graphite-epoxy face	181.0	10.3	10.3	5.96	7.17	7.17	0.40	0.016	0.277
Glass-phenolic honeycomb core	0.032	0.032	0.300	0.048	0.048	0.013	0.25	0.25	0.25

element and method, besides the elasticity, the results are also compared with results from a direct application and closed-form solution of the EHSAPT with improved stiffness constants as given by Eq. (11), as well as the earlier HSAPT theory [4].

The boundary conditions for this simply supported beam are $\tilde{w}^t = \tilde{w}^b = \tilde{w}^c = 0$ at $x = 0$ and $x = a$. Considering that both the geometry and loading are symmetric, the axial displacement should equal to zero at the middle. For convenience, we assume an even number of elements m, which would yield an odd number of nodes, $n = m + 1$; in this case, the boundary conditions are applied as

$$w_1^t = w_1^b = w_1^c = 0 \qquad \text{[first node]} \tag{23a}$$

$$w_n^t = w_n^b = w_n^c = 0 \qquad \text{[last node]} \tag{23b}$$

$$u_{(n+1)/2}^t = u_{(n+1)/2}^b = u_{(n+1)/2}^c = 0 \qquad \text{[middle node]} \tag{23c}$$

Normalized results are given in the following, where the stresses are normalized with q_0 and the displacements are normalized with

$$w_{\text{norm}} = \frac{3q_0 a^4}{2\pi^4 E_1^t f_t^3} \tag{24}$$

Figure 3 gives the normalized transverse displacement of the middle point at the top sheet when different number of elements are used. That point is also the maximum transverse displacement point over the sandwich beam. The number of elements ranges from 2 to 100. Figure 3 shows that the results converge very fast. Parts of the results are listed in Table 2. In addition, the elasticity value and the one from a closed-form analytical solution of the EHSAPT are also listed in Table 2. The relative error is defined with respect to the elasticity value by

$$\text{Relative Error}(\%) = \frac{w_{\max}^t - w_{\text{elasticity}}}{w_{\text{elasticity}}} \times 100\% \tag{25}$$

When only six elements are used, the relative error is less than 0.5%. A two-dimensional (2-D) model is also built and analyzed with the commercial Finite Element Analysis software Abaqus.

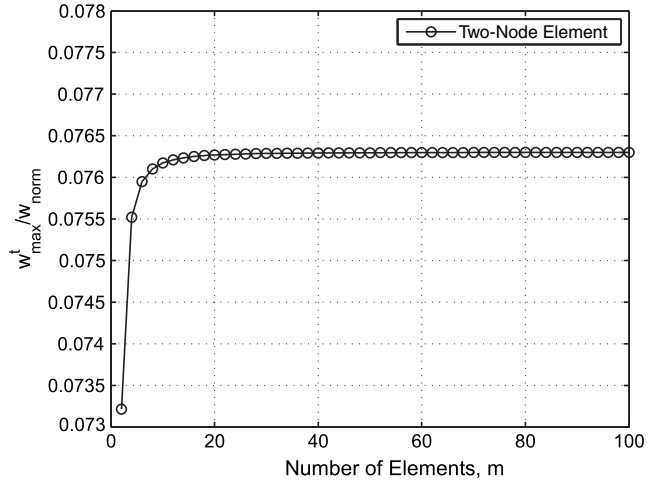

Fig. 3 Transverse displacement of the middle point vs number of elements m.

Table 2 Effect of number of elements on the accuracy

Number of elements	$w_{\max}^t/w_{\text{norm}}$	Relative error, %
2	0.073212512	−3.9889
4	0.075520416	−0.9623
6	0.075946935	−0.4029
8	0.076099586	−0.2028
10	0.076171146	−0.1089
16	0.076249450	−0.0062
30	0.076285671	0.0413
50	0.076294919	0.0534
100	0.076298825	0.0585
EHSAPT	0.076300127	0.0602
Elasticity	0.076254200	— —

Using six elements along the axial direction and eight elements through the thickness (two for the top face, two for the bottom face, and four for the core), there are a total of 48 2-D rectangular elements. The normalized transverse displacement at the middle point of the top face is $w^t/w_{\text{norm}} = 0.074692$, and the relative error is about −2.0%.

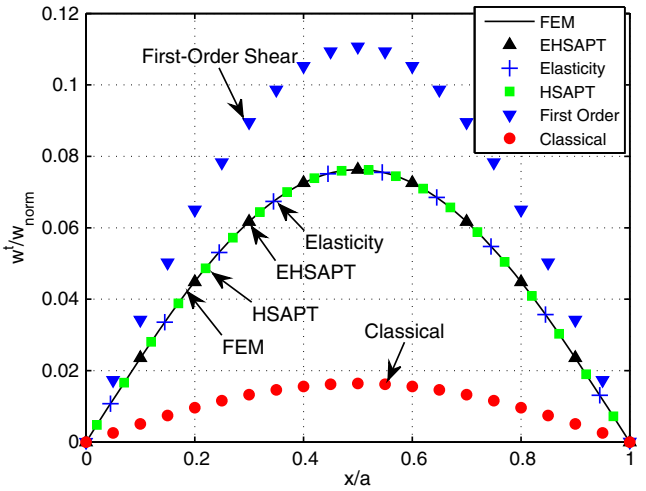

Fig. 4 Transverse displacement at the midpoint of the top face.

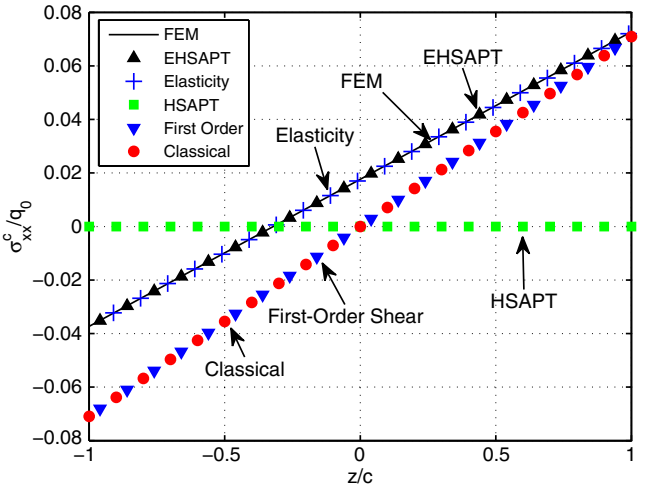

Fig. 5 Through-thickness distribution of the axial stress in the core σ_{xx}^c.

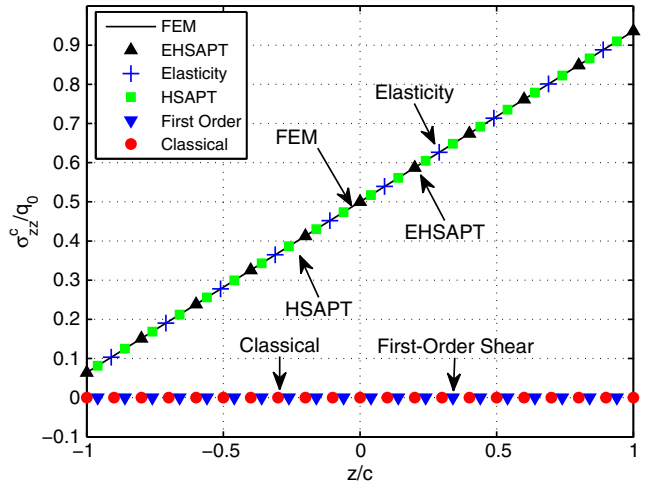

Fig. 6 Through-thickness distribution of the transverse normal stress in the core σ^c_{zz}.

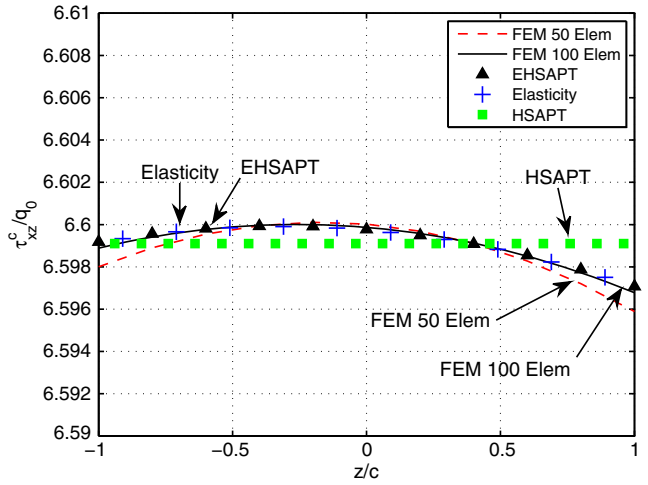

Fig. 7 Through-thickness distribution of the transverse shear stress in the core τ^c_{xz}.

The error is much larger than using the EHSAPT-based element, although the same number of elements is used in the axial direction. Also, it is much easier to build a one-dimensional (1-D) finite element model instead of a 2-D model. Thus, we can conclude that the element is very accurate and efficient.

Figure 4 shows the normalized transverse displacement over the length of the sandwich beam. Results using different methods are plotted in the same figure. "FEM" marks the results obtained by 50 uniform-length two-node 20-DOF EHSAPT-based elements developed in this paper. So, $m = 50$ and $n = 51$. From Fig. 4, it can be seen that the EHSAPT-based finite element solution agrees perfectly with both the elasticity solution and the EHSAPT theory; in this case, the HSAPT is also in agreement. The classical sandwich beam theory assumes that both faces and core obey the Euler–Bernoulli assumption, which implies that the shear modulus is considered to be infinite in both faces and core. This results in overstiffening; the structure and the curve in Fig. 4 are much lower than the elasticity and in significant error. Meanwhile, the first-order shear theory [17], which considers the shear effect of the core, is also inadequate and results in oversoftening of the beam; hence, the displacement predicted is also in considerable error and much higher than the elasticity theory (the latter is regarded as the exact value).

The distribution of the normalized axial stress σ^c_{xx} and normalized transverse stress σ^c_{zz} of the middle point ($x = a/2$) in the core sheet are plotted in Figs. 5 and 6 (50 EHSAPT-based elements are used). Again, the EHSAPT-based element obtained the same results as the EHSAPT theory. These two are exactly the same as the elasticity solution in both the axial and the transverse stresses. It should be noted that the small differences in the axial stress results between EHSAPT and elasticity, which were observed in [5], are not observed now because the core stiffness constants are determined from the more accurate Eq. (11). The HSAPT neglects the in-plane rigid, resulting in a zero axial stress (Fig. 5). Both classical and first-order theories yield a symmetrically distributed axial stress; thus, they cannot capture the offset predicted by elasticity (Fig. 5). From Fig. 6, we can see that the results using the EHSAPT-based element, the EHSAPT theory, the elasticity, and the HSAPT coincide with each other. Since classical theory and first order assume the core to be incompressible, a zero transverse stress is observed with these theories (Fig. 6).

Figure 7 shows the shear stress distribution along the thickness of the core at $x = a/10$. Only the results obtained by the EHSAPT-based element, the closed-form EHSAPT, the elasticity, and the HSAPT are given. Fifty and 100 uniform two-node 20-DOF elements are used in the finite element analysis. The results are marked by "FEM 50 Elem" and "FEM 100 Elem," respectively. In Fig. 7, the error between the 50 uniform two-node 20-DOF elements and the EHSAPT or "elasticity" might seem to be larger than the differences in Figs. 4–6. When considering the scale of the y axis, the maximum relative error between the elasticity solution and the 50 uniform two-node 20-DOF elements is less than -0.02%. When 100 elements are used, the finite element analysis results practically coincide with the elasticity. The HSAPT gives a constant shear stress within the core (Fig. 7). Thus, only with the EHSAPT, or this newly formulated element, can one predict the same parabolic distribution shear stress distribution along the thickness as the elasticity.

Next, one example considering concentrated-load and constrained-only face sheets will be analyzed. The novel sandwich beam element will be shown to be very efficient and capable of solving various combinations of loadings and boundaries.

Example 2: Consider a cantilever sandwich beam with a tip concentrated load, as shown in Fig. 8. The geometric parameters are $a = 254$ mm, $f_t = f_b = 5$ mm, and $c = 19$ mm. The E-glass vinyl ester composite is used in the face sheets, which has Young's modulus $E_1^{t,b} = 13,600$ MPa. The core is isotropic and is made out of Corecell foam with Young's modulus $E^c = 32$ MPa and Poisson's ratio $\nu^c = 0.3$. The tip load is $P = 10$ N per unit width and is applied at the right edge of the top face sheet. In practice, constraints on rotation are only applied to the face sheets for the cantilever sandwich beam. So, the boundary conditions at the first node are expressed as

$$w_1^t = w_1^b = 0 \tag{26a}$$

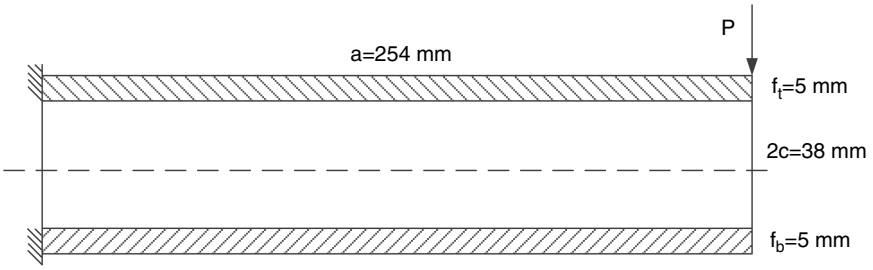

Fig. 8 Sketch of the sandwich cantilever beam (Example 2).

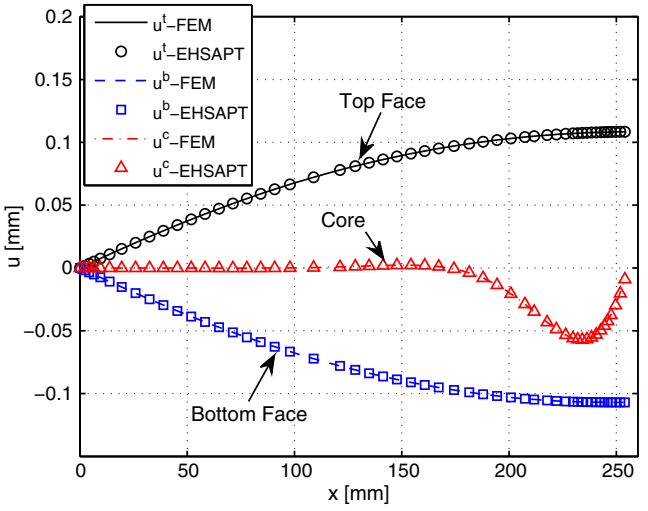

Fig. 9 Axial displacement along the length (cantilever sandwich beam case).

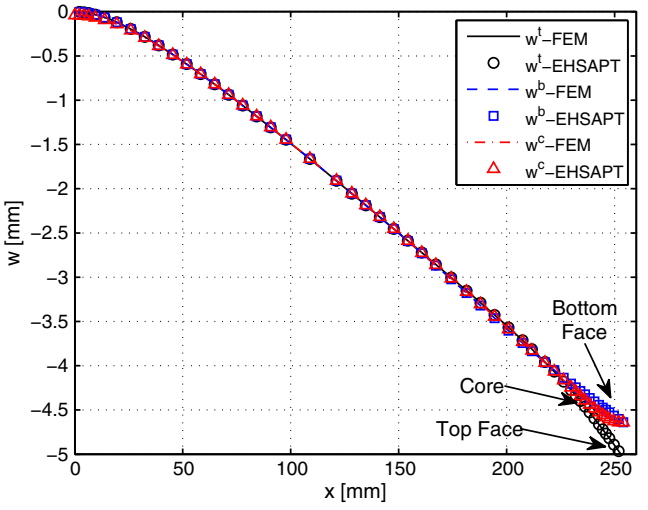

Fig. 10 Transverse displacement along the length (cantilever sandwich beam case).

$$\left(\frac{\mathrm{d}w^t}{\mathrm{d}x}\right)_1 = \left(\frac{\mathrm{d}w^b}{\mathrm{d}x}\right)_1 = 0 \tag{26b}$$

$$u_1^t = u_1^b = 0 \tag{26c}$$

In the FEM analysis, 50 uniform-length two-node 20-DOF elements will be used. So, $m = 50$ and $n = 51$. When using the EHSAPT, the analytical solution is not available for such loading and boundary conditions. To get the results, the seven equilibrium equations need to be further developed to be 18 first-order equations with 18 unknowns. In particular, 9 of the 18 unknowns are the displacements or their first-order derivatives, which are $u_0^{t,b,c}$, $w_0^{t,b,c}$, $w_{0,x}^{t,b}$, and ϕ_0^c. Another nine terms are the corresponding equivalent resultant axial forces, shear forces, and bending moments of the top, core, and bottom sheets. With the variation form of the total potential energy, the equivalent resultant forces and moments are defined by collecting the corresponding coefficients. Also, nine equations that essentially are the first-order derivatives of the equivalent resultant forces in terms of the 18 unknowns can be obtained. Another nine equations are the derivatives of the nine displacement unknowns. With this further derivation, one can establish a first-order ordinary differential equation (ODE) system with boundary conditions either about the displacements or the equivalent resultant forces. Then, a numerical boundary value problem solver in MATLAB is used to solve this first-order ODE system. The solver is a finite difference code and uses a collocation formula, and the collocation polynomial provides a C^1-continuous solution that is fourth-order accurate uniformly in the interval of interest (known as the Lobatto formula). Mesh selection and error control are based on the residual of the continuous solution.

The transverse and axial displacements of the two faces and the core are plotted in Figs. 9 and 10. The results obtained by the FE approach, marked as FEM, and the analytical EHSAPT, marked as EHSAPT, are both given. The novel element yields the same results as the EHSAPT. From Fig. 9, it can be seen that the top face is elongated and the bottom is compressed. It is interesting to notice that the core only shrinks near the loading edge. At the constrained edge, the middle line of the core shows almost no motion in the axial direction. Figure 10 shows that the transverse displacements of the faces and the core are almost the same when they are far away from the loading edge. Near the right edge, the transverse displacement of

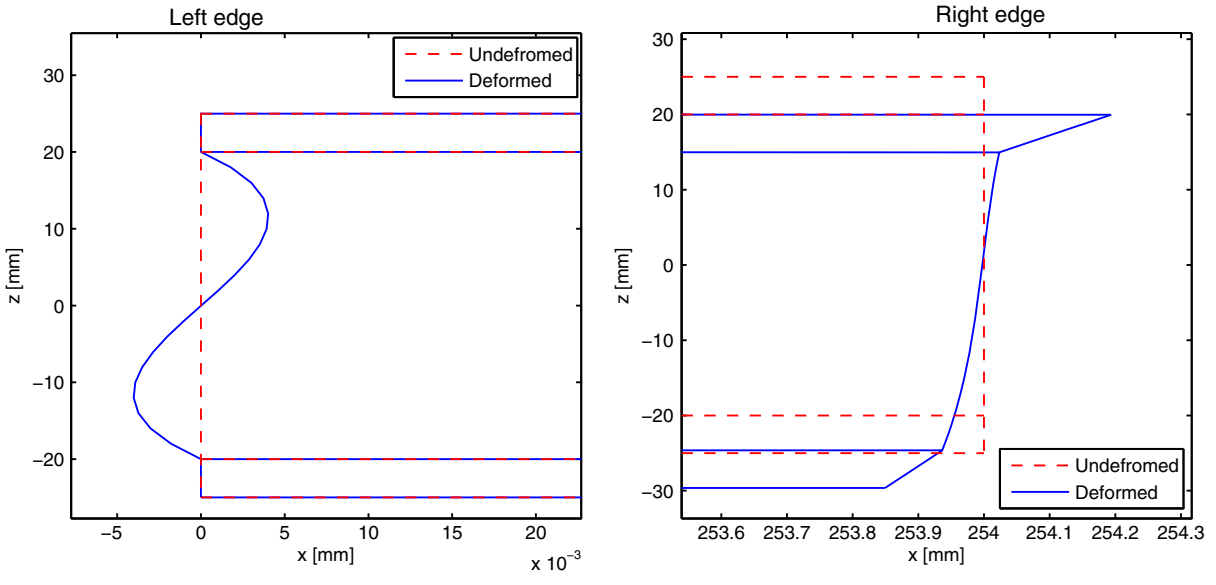

a) b)

Fig. 11 Deformed configuration of the sandwich cantilever beam.

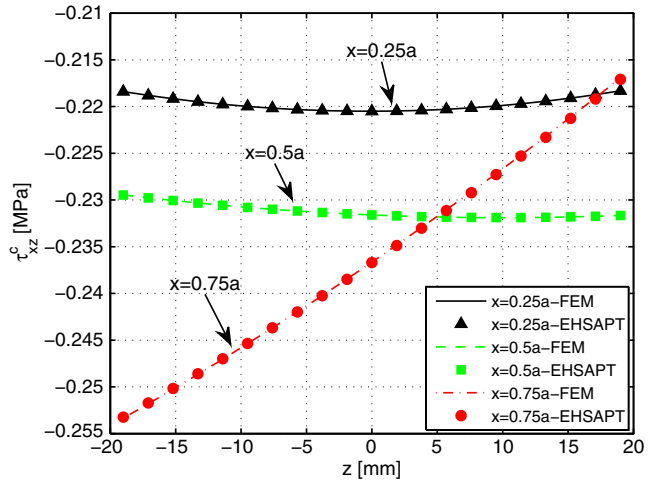

Fig. 12 Through-thickness distribution of the transverse shear stress at various cross sections (cantilever sandwich beam case).

the top face is larger than the bottom face, which reflects the compression in the thickness direction caused by the concentrated load applied at the load, and which is accommodated by the compressible core.

Using Eqs. (1), (2), and (13), the deformed configuration of the whole sandwich beam can be reconstructed with the node displacements obtained from the FEM analysis. Figure 11 shows the deformed shape of the sandwich cantilever beam from the FEM results. To make it clear, only the left edge and the right edge are plotted. The dashed line is the initial configuration, and the solid line is the deformed configuration. Figure 11a (left end) shows that the cross section of the core through the thickness is twisted (it was a straight line before the deformation). The upper part and the lower part move forward and backward, respectively, in Fig. 11b (right end). The displacement assumptions used in the EHSAPT (i.e., Euler–Bernoulli assumptions in the face sheets and higher displacement functions assumed in the core) can be clearly seen in Fig. 11b.

The shear stress distribution at several cross sections is shown in Fig. 12. Both FEM results and EHSAPT results are given. The curves represent the results obtained from the FEM, and the symbols are the results obtained from the EHSAPT. Again, these two results also perfectly agree with each other. The parabolic distributions are well captured by both the EHSPAT and the novel finite element approach. The shear stress shows a more significant variation along the thickness at the region close to the edge.

Conclusions

A novel sandwich beam/wide plate finite element is formulated based on the extended high-order sandwich panel theory, which was recently introduced. The theory makes different assumptions for the displacement profiles of the face sheets and the core. The cross section deformation is described by 10 deg of freedom at each node. The deformed configuration and stress distribution of the whole structures can be reconstructed from the nodal displacements, which involve displacements and rotations of the central surface of the two face sheets and the core. The cross section of the core can deform freely and is not required to remain plane after deformation. The theory employs higher-order terms, and the nonlinear (nearly parabolic) shear stress distribution in the core is well captured. It should be noted that a more accurate way of determining the core stiffness constants is suggested in this paper, and this eliminated the small differences in the axial stress results between the extended high-order sandwich panel theory (EHSAPT) and elasticity, which were observed in [5].

Two static examples involving various combinations of boundary conditions and loading are analyzed to verify the convergence, accuracy, efficiency, and capability of the novel sandwich beam element. The results are compared with analytical solutions from the EHSAPT; elasticity; classical sandwich beam theory; first-order shear theory; and the earlier sandwich panel theory, high-order sandwich panel theory. It shows that the presented finite element can yield great accuracy at very low computational cost. The results always agree with the EHSAPT, for which the results are the closest ones to the elasticity. Unlike the EHSAPT, the novel finite element approach can easily deal with all kinds of loading and boundary conditions.

Acknowledgments

The financial support of the Office of Naval Research (grant N00014-11-1-0597) and the interest and encouragement of the Grant Monitor Y. D. S. Rajapakse are both gratefully acknowledged.

References

[1] Carlsson, L., and Kardomateas, G. A., *Structural and Failure Mechanics of Sandwich Composites*, Springer, New York, 2011.

[2] Wang, E., Gardner, N., and Shukla, A., "The Blast Resistance of Sandwich Composites with Stepwise Graded Cores," *International Journal of Solids and Structures*, Vol. 46, Nos. 18, 19, Sept. 2009, pp. 502–3492.

[3] Kardomateas, G. A., and Phan, C. N., "Three Dimensional Elasticity Solution for Sandwich Beams/Wide Plates with Orthotropic Phases: The Negative Discriminant Case," *Journal of Sandwich Structures and Materials*, Vol. 13, No. 6, Nov. 2011, pp. 641–661. doi:10.1177/1099636211419127

[4] Frostig, Y., Baruch, M., Vilnay, O., and Sheinman, I., "High-Order Theory for Sandwich-Beam Behavior with Transversely Flexible Core," *Journal of Engineering Mechanics*, Vol. 118, No. 5, May 1992, pp. 1026–1043. doi:10.1061/(ASCE)0733-9399(1992)118:5(1026)

[5] Phan, C. N., Frostig, Y., and Kardomateas, G. A., "Analysis of Sandwich Panels with a Compliant Core and with In-Plane Rigidity-Extended High-Order Sandwich Panel Theory Versus Elasticity," *Journal of Applied Mechanics*, Vol. 79, No. 4, 2012, Paper 041001. doi:10.1115/1.4005550

[6] Phan, C. N., Kardomateas, G. A., and Frostig, Y., "Blast Response of a Sandwich Beam/Wide Plate Based on the Extended High-Order Sandwich Panel Theory (EHSAPT) and Comparison with Elasticity," *Journal of Applied Mechanics*, Vol. 80, No. 6, Nov. 2013, Paper 061005. doi:10.1115/1.4023619

[7] Kardomateas, G. A., Frostig, Y., and Phan, C. N., "Dynamic Elasticity Solution for the Transient Blast Response of Sandwich Beams/Wide Plates," *AIAA Journal*, Vol. 51, No. 2, 2013, pp. 485–491. doi:10.2514/1.J051885

[8] Barut, A., Madenci, E., and Tessler, A., "A Refined Zigzag Theory for Laminated Composite and Sandwich Plates Incorporating Thickness Stretch Deformation," *Proceedings of 53rd AIAA/ASME/ASCE/AHS/ASC Structures, Structural Dynamics, and Materials Conference*, AIAA Paper 2012-1705, 2012.

[9] Iurlaro, L., Gherlone, M., and Di Sciuva, M., "A Mixed Cubic Zigzag Model for Multilayered Composite and Sandwich Plates Including Transverse Normal Deformability," *Proceedings of the 11th World Congress on Computational Mechanics (WCCM XI)*, Barcelona, 2014.

[10] Bekuit, J.-J. R. B., Oguamanama, D. C. D., and Damisa, O., "A Quasi-2-D Finite Element Formulation for the Analysis of Sandwich Beams," *Finite Elements in Analysis and Design*, Vol. 43, No. 14, 2007, pp. 1099–1107. doi:10.1016/j.finel.2007.08.005

[11] Oskooei, S., and Hansen, J. S., "Higher-Order Finite Element for Sandwich Plates," *AIAA Journal*, Vol. 38, No. 3, March 2000, pp. 525–533. doi:10.2514/2.991

[12] Hu, H., Belouettar, S., Potier-Ferry, M., and Makradi, A., "A Novel Finite Element for Global and Local Buckling Analysis of Sandwich Beams," *Composite Structures*, Vol. 90, No. 3, 2009, pp. 270–278. doi:10.1016/j.compstruct.2009.02.002

[13] Elmalich, D., and Rabinovitch, O., "A High-Order Finite Element for Dynamic Analysis of Soft-Core Sandwich Plates," *Journal of Sandwich Structures and Materials*, Vol. I4, No. 5, 2012, pp. 525–555.

[14] Long, R., Barry, O., and Oguamanam, D. C. D., "Finite Element Free Vibration Analysis of Soft-Core Sandwich Beams," *AIAA Journal*, Vol. 50, No. 1, Jan. 2012, pp. 235–238. doi:10.2514/1.J050697

[15] Chakrabarti, A., Chalak, H. D., Iqbal, A., and Sheikh, A. H., "A New FE Model Based on Higher Order Zigzag Theory for the Analysis of Laminated Sandwich Beam with Soft Core," *Journal of Composite*

Structures, Vol. 93, No. 2, 2011, pp. 271–279.
doi:10.1016/j.compstruct.2010.08.031

[16] Barut, A., Madenci, E., and Tessler, A., "C0-Continuous Triangular Plate Element for laminated Composite and Sandwich Plates Using the (2,2)-Refined Zigzag Theory," *Composite Structures*, Vol. 106, Dec. 2013, pp. 835–853.
doi:10.1016/j.compstruct.2013.07.024

[17] Carlsson, L., and Kardomateas, G. A., *Structural and Failure Mechanics of Sandwich Composites*, Springer, New York, 2011.

C. Cesnik
Associate Editor